Journal of Zhejiang University SCIENCE
ISSN 1009-3095
http://www.zju.edu.cn/jzus
E-mail: jzus@zju.edu.cn

Mathematical modeling of salt-gradient ion-exchange simulated moving bed chromatography for protein separations*

LU Jian-gang (卢建刚)

(*National Laboratory of Industrial Control Technology, Institute of Industrial Process Control, Zhejiang University, Hangzhou 310027, China*)

E-mail: JGLU@iipc.zju.edu.cn

Received Oct. 8, 2003; revision accepted Feb. 28, 2004

Abstract: The salt-gradient operation mode used in ion-exchange simulated moving bed chromatography (SMBC) can improve the efficiency of protein separations. A detailed model that takes into account any kind of adsorption/ion-exchange equilibrium, salt gradient, size exclusion, mass transfer resistance, and port periodic switching mechanism, was developed to simulate the complex dynamics. The model predictions were verified by the experimental data on upward and downward gradients for protein separations reported in the literature. All design and operating parameters (number, configuration, length and diameter of columns, particle size, switching period, flow rates of feed, raffinate, desorbent and extract, protein concentrations in feed, different salt concentrations in desorbent and feed) can be chosen correctly by numerical simulation. This model can facilitate the design, operation, optimization, control and scale-up of salt-gradient ion-exchange SMBC for protein separations.

Key words: Simulated moving bed chromatography, Salt gradients, Size exclusion, Proteins, Mathematical model
doi:10.1631/jzus.2004.1613 **Document code:** A **CLC number:** O657.7; TQ460.35

INTRODUCTION

Simulated moving bed chromatography (SMBC) had been applied not only to hydrocarbons and sugars, but also to various biotechnological and pharmaceutical mixtures, such as chiral drugs, amino acids and antibiotics (Yu and Ching, 2002; Migliorini *et al.*, 2002). Recent developments in SMBC separation technology applied gradient operation modes (Abel *et al.*, 2004), which include temperature gradients, pressure gradients, and solvent gradients. This work deals with the salt-gradient operation mode during separation of proteins by ion-exchange (Houwing *et al.*, 2002a; 2002b; 2003a; 2003b). The salt gradients were formed by the feed and desorbent solutions of different salt concentrations. Experimental results showed that the thus introduced regions of high and low affinity may reduce the consumption of solvent and sorbent compared to isocratic SMBC.

In general, in a salt-gradient ion-exchange SMBC for protein separations, both mass transfer resistance and size exclusion usually are significant due to the small diffusivities and the large molecules of proteins. And the protein SMBC is preferred to be run at concentrations as high as possible in order to be economically viable, which suggests that it may be done under nonlinear competitive conditions. Furthermore, the adsorption/ion-exchange

* Project supported by the National Natural Science Foundation of China (No. 20206027), the National Basic Research Program (973) of China (No. 2002CB312200), and the Natural Science Foundation of Zhejiang Province (No. 202046), China

equilibrium of proteins is very sensitive to the salt concentration; so the effect of salt gradient must be taken into account simultaneously. Finally, as the characteristic feature of SMBC, the discrete event of port switching should be coupled within the model.

Recently, Protein fixed-bed chromatography often exploits salt-gradient operation mode (Yamamoto *et al.*, 1988) and/or size-exclusion effect (Gao *et al.*, 2003) to increase the resolution and productivity and various models are available to describe its behavior (Yamamoto *et al.*, 1988; Gu, 1995). However, mathematical modeling of salt-gradient ion-exchange SMBC for protein separation prior to plant operation is very difficult, due to the complexity of the SMBC process. The "equilibrium theory" model and the so-called "triangle theory" neglect axial dispersion and mass-transfer resistance and hence assume infinite column efficiency (Houwing *et al.*, 2002a; 2002b; Abel *et al.*, 2004). The equilibrium stage (true moving bed approximation) model should adjust the number of equilibrium stages to match mass-transfer and dispersive effects (Houwing *et al.*, 2003a). The steady-state equivalent true moving bed model incorporates mass-transfer effects, but it was developed for isocratic SMBC, with salt gradients not being involved (Houwing *et al.*, 2003b). All these models available in the literature assume linear isotherms, which suggest the dilute mixtures of proteins are separated without any interference phenomena (Houwing *et al.*, 2002a; 2002b; 2003a; 2003b). They can give the initial values of design parameters and operating conditions, but cannot give a detailed quantitative analysis due to unrealistic model simplifications and assumptions.

Comparatively speaking, mathematical models available in the literature of SMBC in the isocratic mode are more detailed. In the detailed SMBC models (Silva *et al.*, 2002; Minceva *et al.*, 2003; Pais and Rodrigues, 2003), the intraparticle mass-transfer rate is described by linear driving force (LDF) approximation because of its simplicity. More recently, the non-linear non-ideal models of SMBC with detailed intraparticle mass-transfer and adsorption mechanisms were developed by Hritzko *et al.*(2002) and Lu (2003).

The objective of this work is to extend the detailed non-linear non-ideal model of isocratic SMBC to the salt-gradient ion-exchange SMBC, which takes into account any kind of adsorption/ion-exchange equilibrium, salt gradient, size exclusion, mass transfer resistance, and port periodic switching mechanism simultaneously, and to gain insight into the complex dynamics.

MODELING

The physical configuration of an SMBC is a set of fixed-bed chromatographic columns connected in series segmented by valves and inlet/outlet lines (Yu and Ching, 2002; Migliorini *et al.*, 2002), as illustrated in Fig.1. It is characterized by shifting periodically the inlet/outlet lines equally in the direction of fluid-phase flow to simulate countercurrent motion of the sorbent. SMBC normally consists of four sections. If columns between desorbent (D) and extract (E) lines are defined as section I, then columns between extract (E) and feed (F) lines are section II, columns between feed (F) and raffinate (R) lines are section III, and columns between raffinate (R) and desorbent (D) lines are section IV. Usually ion-exchange SMBC is operated using the open loop mode. The salt-gradient ion-exchange SMBC model is a system of all the single column models coupled with all the node models.

Node model

The volumetric flow rate (Q) and fluid phase concentration (c) of each section inlet at the corresponding node are derived from mass balance and given by the equations in Table 1. The interstitial velocity (u_0) in each section is $4Q/\pi d^2\varepsilon$.

Single column model

Using the dimensionless axial axis (x), the dimensionless particle radial axis (ρ), and the interstitial velocity (u_0), the following differential equations of mass balance for component j in the

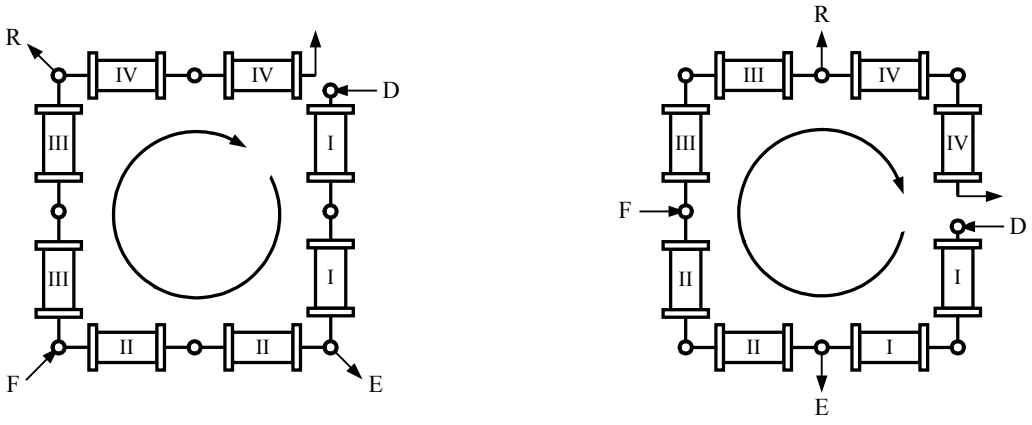

Fig.1 Schematic representation of an open loop SMBC with two columns in each section
(a): this switching period; (b): next switching period

Table 1 Node model equations

Node name	Volumetric flow rate (cm^3/min)	Concentration (g/L)
Desorbent node	$Q_{\mathrm{I}} = Q_{\mathrm{D}}$	$c_{j,\mathrm{I}}^{\mathrm{in}} = c_{j,\mathrm{D}}$
Extract node	$Q_{\mathrm{II}} = Q_{\mathrm{I}} - Q_{\mathrm{E}}$	$c_{j,\mathrm{II}}^{\mathrm{in}} = c_{j,\mathrm{I}}^{\mathrm{out}}$; $c_{j,\mathrm{E}} = c_{j,\mathrm{I}}^{\mathrm{out}}$
Feed node	$Q_{\mathrm{III}} = Q_{\mathrm{II}} + Q_{\mathrm{F}}$	$c_{j,\mathrm{III}}^{\mathrm{in}} = \dfrac{Q_{\mathrm{II}} c_{j,\mathrm{II}}^{\mathrm{out}} + Q_{\mathrm{F}} c_{j,\mathrm{F}}}{Q_{\mathrm{III}}}$
Raffinate node	$Q_{\mathrm{IV}} = Q_{\mathrm{III}} - Q_{\mathrm{R}}$	$c_{j,\mathrm{IV}}^{\mathrm{in}} = c_{j,\mathrm{III}}^{\mathrm{out}}$; $c_{j,\mathrm{R}} = c_{j,\mathrm{III}}^{\mathrm{out}}$

fluid phase [Eq.(1)] and particle phase [Eq.(2)] can be obtained

$$\frac{\partial c_j}{\partial t} = \frac{D_{\mathrm{L}j}}{L^2}\frac{\partial^2 c_j}{\partial x^2} - \frac{u_0}{L}\frac{\partial c_j}{\partial x} - \frac{3(1-\varepsilon)k_{\mathrm{f}j}}{\varepsilon R_{\mathrm{p}}}(c_j - c_{\mathrm{p}j,\rho=1}) \quad (1)$$

$$\varepsilon_{\mathrm{p}j}\frac{\partial c_{\mathrm{p}j}}{\partial t} + (1-\varepsilon_{\mathrm{p}j})\frac{\partial \overline{c}_{\mathrm{p}j}}{\partial t} = \frac{\varepsilon_{\mathrm{p}j} D_{\mathrm{p}j}}{R_{\mathrm{p}}^2}\frac{1}{\rho^2}\frac{\partial}{\partial \rho}\left(\rho^2 \frac{\partial c_{\mathrm{p}j}}{\partial \rho}\right) \quad (2)$$

with boundary conditions:

$$\frac{\partial c_j}{\partial x} = \frac{u_0 L}{D_{\mathrm{L}j}}(c_j - c_j^{\mathrm{in}}), \quad t > 0, \quad x = 0 \quad (3)$$

$$\frac{\partial c_j}{\partial x} = 0, \quad t > 0, \quad x = 1 \quad (4)$$

$$\frac{\partial c_{\mathrm{p}j}}{\partial \rho} = 0, \quad t > 0, \quad \rho = 0 \quad (5)$$

$$\frac{\partial c_{\mathrm{p}j}}{\partial \rho} = \frac{k_{\mathrm{f}j} R_{\mathrm{p}}}{D_{\mathrm{p}j}}(c_j - c_{\mathrm{p}j}), \quad t > 0, \quad \rho = 1 \quad (6)$$

and initial conditions:

$$c_j = c_j(0,x), \quad t = 0, \quad x \in [0,1] \quad (7)$$

$$c_{\mathrm{p}j} = c_{\mathrm{p}j}(0,\rho), \quad t = 0, \quad \rho \in [0,1] \quad (8)$$

It should be pointed out that in Eq.(2) an "accessible intraparticle porosity (ε_{p})" is introduced to take the size exclusion effect into account. The adsorption concentration of component j in the particle phase ($\overline{c}_{\mathrm{p}j}$), which is assumed to be in equilibrium with the concentrations of all NC components in the local pore liquid ($c_{\mathrm{p}i}$), is based on the fraction of the particle volume inaccessible to component j. Any kind of adsorption isotherm or ion-exchange equilibrium can be handled by these model equations (Lu and Wu, 1997).

SMBC model

The SMBC model is obtained by all the single column models connected in series by Eq.(3). The dominating parameters of the interstitial velocity

(u_0) and the inlet concentration (c_j^{in}) in Eq.(1) and Eq.(3) of each column are given by node model equations in Table 1.

ALGORITHM

The method of orthogonal collocation on finite elements outlined in detail by Finlayson (1980) was proven very efficient for solving fixed-bed chromatography problem (Yu and Wang, 1989; Gu *et al.*, 1990; Gu, 1995; Lu, 1995; Kaczmarski *et al.*, 1997). Here we give a brief description of applying this numerical technique to discretize the model equations in order to introduce our new strategy called "orthogonal collocation on finite elements with periodic movement of concentration vector".

Discretization equations of fluid phase

The dimensionless axial space coordinate for each column is divided into *NE* elements as $0=X_1<X_2<\ldots<X_{NE}<X_{NE+1}=1$. Then the first order discretization matrix $\boldsymbol{A}$ and the second order discretization matrix $\boldsymbol{B}$, derived from the *NP*th order Legendre orthogonal polynomials defined in the interval [0, 1], are used to discretize the differential equations of fluid phase on each finite element.

Table 2 Model parameters used in simulations

Component	1=NaCl	2=BSA	3=MYO
Mass transfer parameters			
Molecular diffusivity (D_m, cm^2/min)	9.98×10^{-4}	3.60×10^{-5}	6.48×10^{-5}
Intraparticle diffusivity (D_p, cm^2/min)	Eq.(15)	$0.73D_m$	$0.84D_m$
Film mass transfer coefficient (k_f, cm/min)	Eq.(16)	Eq.(16)	Eq.(16)
Axial dispersion coefficient (D_L, cm^2/min)	Eq.(17)	Eq.(17)	Eq.(17)
Thermodynamic parameters			
Isotherm ($\bar{c}_p$)	$0.11\left(\sqrt{1+90c_1^2}-1\right)$ (mol/L)	$\left(0.00161c_1^{-5.61}\right)c_3$ (g/L)	$\left(0.076c_1^{-1.31}\right)c_2$ (g/L)
Design parameters			
Column number (n)	8		
Column configuration (I-II-III-IV)	2–2–2–2		
Column length (L, cm)	9.04		
Column diameter (d, cm)	1.0		
Particle size (R_p, cm)	45.0×10^{-4}		
Bed void fraction (ε)	0.39		
Accessible intraparticle porosity (ε_p)	0.978	0.49	0.64
Operating parameters (RUN 1: upward gradients)			
Desorbent concentration (c_D)	0.27 mol/L	0	0
Feed concentration (c_F)	0.15 mol/L	0.5 g/L	0.1 g/L
Switching period (t_S, min)	4.182		
Desorbent flow rate (Q_D, cm^3/min)	2.94		
Extract flow rate (Q_E, cm^3/min)	1.03		
Feed flow rate (Q_F, cm^3/min)	2.02		
Raffinate flow rate (Q_R, cm^3/min)	2.05		
Operating parameters (RUN 2: downward gradients)			
Desorbent concentration (c_D)	0.22 mol/L	0	0
Feed concentration (c_F)	0.31 mol/L	0.5 g/L	0.1 g/L
Switching period (t_S, min)	2.515		
Desorbent flow rate (Q_D, cm^3/min)	2.77		
Extract flow rate (Q_E, cm^3/min)	0.26		
Feed flow rate (Q_F, cm^3/min)	0.19		
Raffinate flow rate (Q_R, cm^3/min)	1.53		

$x\in(X_k, X_{k+1})$:

$$\frac{\mathrm{d}c_{j,IX}}{\mathrm{d}t}=\frac{D_{\mathrm{L}j}}{L^2}\frac{1}{(X_{k+1}-X_k)^2}\sum_{J=1}^{NP+2}B_{IX,J}c_{j,J}-\frac{u_0}{L}\frac{1}{(X_{k+1}-X_k)}\sum_{J=1}^{NP+2}A_{IX,J}c_{j,J}-\frac{3(1-\varepsilon)k_{\mathrm{f}j}}{\varepsilon R_{\mathrm{p}}}(c_{j,IX}-c_{\mathrm{p}j,\rho=1})$$
$$(IX=2,3,\cdots,NP+1) \quad (9)$$

x=0:

$$\sum_{J=1}^{NP+2}A_{1,J}c_{j,J}=\frac{u_0L}{D_{\mathrm{L}j}}(c_{j,1}-c_j^{\mathrm{in}}) \quad (10)$$

$x=X_k$:

$$(c_{j,NP+2})_{\text{element }k-1}=(c_{j,1})_{\text{element }k},$$
$$\left(\frac{1}{(X_k-X_{k-1})}\sum_{J=1}^{NP+2}A_{(NP+2),J}c_{j,J}\right)_{\text{element }k-1}=\left(\frac{1}{(X_{k+1}-X_k)}\sum_{J=1}^{NP+2}A_{1,J}c_{j,J}\right)_{\text{element }k}$$
$$(k=2,3,\cdots,NE) \quad (11)$$

x=1:

$$\sum_{J=1}^{NP+2}A_{(NP+2),J}c_{j,J}=0 \quad (12)$$

Discretization equations of particle phase

The particle phase differential equations are discretized through the first order discretization matrix $\bar{\boldsymbol{A}}$ and the second order discretization matrix $\bar{\boldsymbol{B}}$, which are derived from the (2×*NPR*)th Jacobian orthogonal polynomials defined in ρ^2

$$(1-\varepsilon_{\mathrm{p}j})\sum_{i=1}^{NC}\left(\frac{\partial\bar{c}_{\mathrm{p}j,IP}}{\partial c_{\mathrm{p}i,IP}}\frac{\partial c_{\mathrm{p}i,IP}}{\partial t}\right)+\varepsilon_{\mathrm{p}j}\frac{\mathrm{d}c_{\mathrm{p}j,IP}}{\mathrm{d}t}=\frac{\varepsilon_{\mathrm{p}j}D_{\mathrm{p}j}}{R_{\mathrm{p}}^2}\sum_{J=1}^{NPR+1}\bar{B}_{IP,J}c_{\mathrm{p}j,J}$$
$$(IP=1,2,\cdots,NPR) \quad (13)$$

ρ=1:

$$\sum_{J=1}^{NPR+1}\bar{A}_{NPR+1,J}c_{\mathrm{p}j,J}=\frac{k_{\mathrm{f}j}R_{\mathrm{p}}}{D_{\mathrm{p}j}}(c_j-c_{\mathrm{p}j,NPR+1}) \quad (14)$$

The algebraic Eqs.(10) to (12) and Eq.(14) can be used to eliminate the corresponding number of unknowns from the ODEs Eqs.(9) and (13). Then the obtained complex ODEs system is integrated simultaneously by Gear's stiff method.

In the SMBC process, the periodic port switching results in sudden changes of the interstitial velocity (u_0), the boundary conditions (c_j^{in}) and the initial conditions for each column. Generally, we have to repeat reconstructing the complex ODEs system when port switching takes place. To avoid repeating this tedious reconstructing task, we presented a new strategy called periodic movement of concentration vector. The idea is based on the fact that the case of a simulated moving bed achieved by port switching in the direction of fluid-phase flow, as illustrated in Fig.1, is equivalent to that of fixing the four ports of streams of feed, raffinate, desorbent and extract (i.e. no port switching) while moving each column periodically by a step of column length in the negative direction of fluid-phase flow. We conclude that moving the concentration vector of all collocation points in each column, including the concentrations of fluid phase (c) and the corresponding concentrations of particle phase (c_p), by a step of column length in the negative direction of fluid-phase flow, can simulate the port switching mechanism without reconstructing the ODEs system, since only the initial conditions of each column is replaced by that of the neighboring downstream column. This new strategy makes the numerical solution technique more efficient.

In this work, numerical parameters used for each column are six finite elements and six interior collocation points per element for fluid phase and three interior collocation points for particle phase (i.e., *NE*=6, *NP*=6, *NPR*=3). In order to avoid the numerical oscillation resulting from Eq.(3), finite elements are preferably concentrated on the inlet region of each column, illustrated as [X_1, X_2, X_3, X_4, X_5, X_6, X_7]=[0, 0.001, 0.01, 0.25, 0.50, 0.75, 1.0].

SIMULATION RESULTS AND DISCUSSION

The separation of bovine serum albumin (BSA) and myoglobin (MYO) by using an ion-exchange

SMBC on Q-Sepharose FF in 10 mmol/L Tris buffer at pH 8 with salt gradient operation and size exclusion effect is used as a model system in this work.

Model parameters

All model parameters used in simulations are summarized in Table 2 (Houwing *et al.*, 2002b; 2003b). Mass transfer parameters such as k_f, D_L, D_p are often not available from literature, or not easily measured by experiment. However, they can be estimated from standard correlations with certain accuracy. The estimation of the intraparticle diffusivity D_p for BSA or MYO from the molecular diffusivity D_m is available (Houwing *et al.*, 2002b; 2003b). For small ions, D_p of salt (NaCl) can be estimated from a correlation obtained by Helfferich (1983),

$$D_{p,1}=\left(\frac{\varepsilon_{p,1}}{2-\varepsilon_{p,1}}\right)^2 D_{m,1} \tag{15}$$

The following correlation may be used to obtain the film mass transfer coefficient k_f (Gu, 1995),

$$Sh=2.0+1.45Sc^{1/3}Re^{0.5} \quad (Re<100) \tag{16}$$

where $Sh=2R_pk_f/D_m$, $Sc=\mu/(\rho D_m)$, and $Re=2R_p\rho u_0/\mu$. μ is the fluid (water) viscosity, and ρ is the fluid density.

The axial dispersion coefficient D_L can be estimated from the following correlation (Gu, 1995),

$$D_L=\frac{2R_pu_0\varepsilon}{0.2+0.011Re^{0.48}} \tag{17}$$

Verification of the salt-gradient ion-exchange SMBC model for protein separations

Upward gradients and downward gradients are two kind of salt-gradient operation modes usually exploited in ion-exchange SMBC for protein separations. In upward gradients, salt is predominantly transported by the fluid in the direction of section I to section IV. In downward gradients, salt is predominantly transported by the sorbent in the direction of section IV to section I. Dynamic behaviors of the salt-gradient ion-exchange SMBC with both upward gradients and downward gradients are predicted by this model using the parameters summarized in Table 2.

Fig.2a shows the axial concentration profile at half switch time of salt-gradient ion-exchange SMBC for protein separations after the cyclic steady state is approached, where upward gradient operating parameters (RUN 1) are used. The predicted purities are 99.85% for BSA in extract and 92.97% for MYO in raffinate. Houwing *et al.*(2002b) gave a qualitative insight into the movement behavior of each component on the basis of equilibrium theory, but failed in understanding why the anticipated movement of BSA in section I was upward whereas downward movement was observed in experiment. It is interesting that Fig.2a allows for a quantitative analysis of this controversial phenomenon. This can be explained by the mass-transfer effects, where small intraparticle diffusivities of proteins play an important role. It must be pointed out that since the experimental points is the data determined between two neighboring columns (Houwing *et al.*, 2002b), the real axial concentration profile can be expected to be more complicated than the experimental profile and may be in closer agreement with the model prediction.

Fig.2b shows the axial concentration profile at half switch time of salt-gradient ion-exchange SMBC for protein separations after the cyclic steady state is approached, where downward gradient operating parameters (RUN 2) are applied and complete separation of BSA and MYO did not occur. The model prediction also gives a quantitative insight into the controversial phenomenon that the movement of MYO in section III is predicted upward by Houwing *et al.*(2002b) whereas the observed movement of MYO was predominantly downward.

However, it can be found that the axial concentration profiles of MYO in section II as shown in Fig.2a and in section I as shown in Fig.2b are slightly more retained than the experimental data. The competition of proteins for sorbent sites (interference effect) may have a contribution. It can be

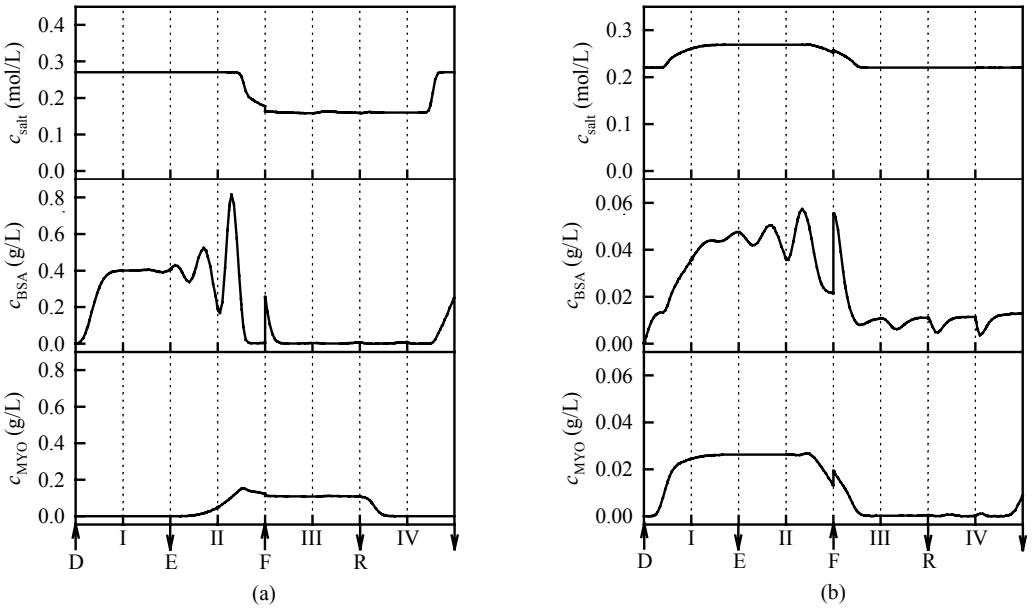

Fig.2 Model prediction of axial concentration profile at half switch time of salt-gradient ion-exchange SMBC for protein separations (a) upward gradient; (b) downward gradient

expected that if the adsorption isotherm or ion-exchange equilibrium takes the non-linear competitive effects between different proteins into account, the model predictions of MYO profile will be much closer to the experimental data.

CONCLUSION

Obviously, to design and operate a salt-gradient ion-exchange SMBC for protein separations, many parameters (number, configuration, length and diameter of columns, particle size, switching period, flow rates of feed, raffinate, desorbent and extract, protein concentrations in feed, different salt concentrations in desorbent and feed) must be chosen correctly. Empirical approaches are too time consuming and expensive. Mathematical models available in literature (Houwing *et al.*, 2002a; 2002b; 2003a; 2003b) lack sufficient accuracy for quantitative analysis of the effects of all the above parameters on SMBC performance, due to the unrealistic and crude modeling assumptions.

The detailed model that takes into account any kind of adsorption/ion-exchange equilibrium, salt-gradient, size-exclusion, mass transfer resistance, and port periodic switching mechanism, was developed to investigate the effects of all these parameters on SMBC performance. The model predictions were verified by the experimental data of both upward gradients and downward gradients for protein separations reported in the literature (Houwing *et al.*, 2002b). Furthermore, because mass transfer parameters such as k_f and D_L are given by the correlations which take into account particle size and interstitial velocity, it can be expected that the detailed SMBC model will be a powerful and accurate tool for optimization and scale-up, when different flow rates are selected and different particle size are compared. Finally, it should be emphasized that the detailed model can handle any kind of adsorption isotherm or ion-exchange equilibrium, which suggests that it has the potential of describing the competition of different proteins for sorbent sites when high concentration mixtures of proteins are to be separated.

It can be concluded that this detailed model can facilitate the design, operation, optimization, control and scale-up of salt-gradient ion-exchange SMBC for protein separations. Since this detailed

model is somewhat more computation-time consuming than the "equilibrium theory" model (Houwing *et al.*, 2002a; 2002b), the most reasonable way is to use the "triangle theory" to obtain a rough separation region of design and operation parameters (Houwing *et al.*, 2002a; 2002b), and then to use this detailed model and the numerical technique to find the most suitable parameters by multiobjective optimization strategy (Zhang *et al.*, 2002) of non-dominated sorting genetic algorithm (NSGA), which is under investigation in our laboratory.

References

Abel, S., Mazzotti, M., Morbidelli, M., 2004. Solvent gradient operation of simulated moving beds 2. Langmuir isotherms. *J. Chromatography A*, **1026**:47-55.

Finlayson, B.A., 1980. Non-linear Analysis in Chemical Engineering. McGraw-Hill, New York.

Gao, Y.G., Guan, Y.X., Yao, S.J., Cho, M.G., 2003. Lysozyme refolding at high concentration by dilution and size-exclusion chromatography. *J. Zhejiang University SCIENCE*, **4**(2):136-141.

Gu, T., 1995. Mathematical Modeling and Scale-up of Liquid Chromatography. Springer, Berlin.

Gu, T., Tsai, G.J., Tsao, G.T., 1990. New approach to a general nonlinear multicomponent chromatography model. *AIChE J.*, **36**:784-788.

Helfferich, F.G., 1983. Ion-exchange Kinetics–Evolution of A Theory. *In*: Liberti, L., Helfferich, F.G. (Eds.), Mass Transfer and Kinetics of Ion-exchange (NATO ASI Series E: Applied Science, No. 71). Martinus Nijhoff, The Hague, p.162.

Houwing, J., Billiet, H.A.H., van der Wielen, L.A.M., 2002a. Optimization of azeotropic protein separations in gradient and isocratic ion-exchange simulated moving bed chromatography. *J. Chromatography A*, **944**:189-201.

Houwing, J., van Hateren, S.H., Billiet, H.A.H., van der Wielen, L.A.M., 2002b. Effect of salt gradients on the separation of dilute mixtures of proteins by ion-exchange in simulated moving beds. *J. Chromatography A*, **952**:85-98.

Houwing, J., Jensen, T.B., van Hateren, S.H., Billiet, H.A.H., van der Wielen, L.A.M., 2003a. Positioning of salt gradients in ion-exchange SMB. *AIChE J.*, **49**:665-674.

Houwing, J., Billiet, H.A.H., van der Wielen, L.A.M., 2003b. Mass-transfer effects during separation of proteins in SMB by size exclusion. *AIChE J.*, **49**:1158-1167.

Hritzko, B.J., Xie, Y., Wooley, R.J., Wang, N.H.L., 2002. Standing-wave design of tandem SMB for linear multicomponent systems. *AIChE J.*, **48**:2769-2787.

Kaczmarski, K., Mazzotti, M., Storti, G., Morbidelli, M., 1997. Modeling fixed-bed adsorption columns through orthogonal collocations on moving finite elements. *Comput. Chem. Eng.*, **21**:641-660.

Lu, J.G., 1995. Preparative Ion-Exchange Chromatography of Amino Acids. Ph. D. Thesis, Chem. Eng. Dept., Zhejiang Univ., Hangzhou (in Chinese).

Lu, J.G., 2003. A non-linear non-ideal model of simulated moving bed chromatography for chiral separations. *Chinese J. Chem. Eng.*, **11**:234-239.

Lu, J.G., Wu, P.D., 1997. Dynamics of preparative ion-exchange chromatography of amino acids. *J. Chem. Eng. Chinese Univ.*, **11**:163-165 (in Chinese).

Migliorini, C., Mazzotti, M., Zenoni, G., Morbidelli, M., 2002. Shortcut experimental method for designing chiral SMB separations. *AIChE J.*, **48**:69-77.

Minceva, M., Pais, L.S., Rodrigues, A.E., 2003. Cyclic steady state of simulated moving bed processes for enantiomers separation. *Chem. Eng. Proc.*, **42**:93-104.

Pais, L.S., Rodrigues, A.E., 2003. Design of simulated moving bed and Varicol processes for preparative separations with a low number of columns. *J. Chromatography A*, **1006**:33-44.

Silva, E.A.B., Souza, A.A.U., Souza, S.M.A.G.U., 2002. The use of simulated moving bed in chromatographic separations: Study of the SMB configuration. *Sep. Sci. Technol.*, **37**:1489-1504.

Yamamoto, S., Nakanishi, K., Matsuno, R., 1988. Ion-Exchange Chromatography of Proteins. Marcel-Dekker, New York and Basel.

Yu, H.W., Ching, C.B., 2002. Optimization of a simulated moving bed based on an approximated Langmuir model. *AIChE J.*, **48**:2240-2246.

Yu, Q., Wang, N.H.L., 1989. Computer simulations of multicomponent ion exchange and adsorption in fixed beds–Gradient-directed moving finite element method. *Comput. Chem. Eng.*, **13**:915-926.

Zhang, Z.Y., Hidajat, K., Ray, A.K., Morbidelli, M., 2002. Multiobjective optimization of SMB and varicol process for chiral separation. *AIChE J.*, **48**:2800-2816.